# Measurements of Dibosons with the ATLAS Detector and Associated Constraints on New Physics

Michael Kagan, On Behalf of the ATLAS Collaboration

*Harvard University*
*mkagan@cern.ch*

**Abstract.** Diboson cross sections have been measured for the $W\gamma$, $Z\gamma$, $WW$, $WZ$, and $ZZ$ processes by the ATLAS experiment in $pp$ collisions at $\sqrt{s} = 7$ TeV at the LHC. The cross sections are measured in kinematic regions defined by the decay kinematics, in some cases including vetoes on additional jets. The measurements are also extrapolated to the full phase space using theoretical calculations of the acceptance, and are additionally used to place constraints on triple gauge boson couplings.

**Keywords:** ATLAS, LHC, Dibosons, Electroweak Physics, Anomalous Triple Gauge Couplings
**PACS:** 12.15.-y, 12.60.Cn, 14.70.Fm,14.70.Hp, 14.70.Bh

ATL-PHYS-PROC-2012-139
22 August 2012

## INTRODUCTION

Precise measurements of diboson production test the high energy behavior of the Electroweak (EW) sector of the Standard Model (SM). Triple gauge boson interactions, which are fixed in the SM by the EW gauge structure, play an important role in diboson production. Any deviation of the gauge boson couplings from gauge constraints will cause significant enhancement of the production cross section at high diboson invariant mass and could indicate the presence of new phenomena involving gauge bosons. These diboson processes, especially $WW$ and $ZZ$, are also important backgrounds to Standard Model Higgs production.

The measurements presented here are performed using ATLAS [1], a general-purpose detector at the Large Hadron Collider (LHC) [2], and use between 1 and 5 fb$^{-1}$ of data from $pp$ collisions at $\sqrt{s} = 7$ TeV collected in 2011. Measurements of total production cross sections and production cross sections in phase space regions defined by decay kinematics, or fiducial cross sections, for the $W\gamma$, $Z\gamma$, $WW$, $WZ$, and $ZZ$, processes are described. All analyses make use of the fully leptonic decay channels of the $W$ and $Z$ bosons. In the following $l$ indicates either an electron or a muon, emission of neutrino(s) is identified by significant missing transverse energy.

## SELECTION

Leptons, consistent with originating from the decay of a $W$ or $Z$ boson, are required to have transverse momentum, $p_T$, larger than 7 to 20 GeV, depending on the analysis, within the region of pseudorapidity $|\eta| < 2.47$ for electrons (excluding the transition region between barrel and end cap calorimeters of $1.37 < |\eta| < 1.52$) and $|\eta| < 2.4$ for muons. Furthermore, to reject leptons produced in the fragmentation of jets, leptons are required to be isolated, i.e. large amounts of energy, as measured by calorimeter energy depositions or tracks, must not be found near the leptons. Photons are required to have a transverse energy $E_T > 15$ GeV, $|\eta| < 2.37$ (excluding the region of $1.37 < |\eta| < 1.52$), and be isolated. Jets are built by clustering energy depositions in the calorimeter using the anti-$k_T$ algorithm [3] with radius parameter 0.4 and are required to have $E_T > 25$ GeV. Finally, as neutrinos do not interact with the detector, their presence is inferred by the apparent lack of momentum conservation in the plane perpendicular to the LHC beamline. This transverse missing energy ($E_T^{miss}$) is defined as the energy needed to restore momentum conservation in the transverse plane, and is calculated using reconstructed physics objects (i.e. leptons, photons, and jets) and calorimeter energy depositions not associated to physics objects. In cases where multiple neutrinos are expected to be present in the event, projections of the missing energy onto the direction of other physics objects can be used to reject backgrounds, as will be discussed in the $WW \rightarrow l\nu l\nu$ and $ZZ \rightarrow ll\nu\nu$ analyses below. Additionally, the angular distance between two objects in the $\eta - \phi$ plane is calculated as $\Delta R = \sqrt{\Delta\phi^2 + \Delta\eta^2}$.

## CROSS SECTION MEASUREMENTS

Total production cross sections are calculated as

$$\sigma_{tot} = \frac{N_{obs} - N_{bkg}}{A \times C \times BR \times \int \mathscr{L} \mathrm{d}t} \tag{1}$$

where $N_{obs}$ is the number of observed events passing the selection, $N_{bkg}$ is the estimated number of background events passing the selection, $A$ is the acceptance which is calculated as the fraction of events falling in the fiducial phase space that includes the cuts on kinematic variables used to select events in the analysis, $C$ is the efficiency to reconstruct and select events that fall in the fiducial phase space, $BR$ is the branching ratio, and $\int \mathscr{L} \mathrm{d}t$ is the integrated luminosity. The acceptance $A$ thus extrapolates from the fiducial to the total phase space, and this extrapolation is sensitive to potentially large theoretical uncertainties. Therefore in addition to total cross sections, fiducial cross sections are measured only within the fiducial phase space without the extrapolation[1].

The production of $W$ and $Z$ bosons in association with a high $p_T$ photon have the highest production cross section of the diboson processes and have been measured at ATLAS [4]. The events are selected by requiring an isolated photon with $p_T > 15$ GeV. $W$ boson candidates are selected by requiring a lepton with $p_T > 25$ GeV, missing energy $E_T^{miss} > 25$ GeV, and a transverse mass[2] satisfying $m_T > 40$ GeV. $Z$ boson candidates are selected by requiring two same-flavor opposite-charge (SFOC) leptons with $p_T > 25$

---

[1] In addition, the branching ratio is not included in the fiducial cross section calculation as the fiducial phase space includes cuts on final state objects and thus defined after all decays.

[2] Transverse mass is defined as $m_T = \sqrt{2 p_T^l E_T^{miss} \times (1 - \cos\Delta\phi)}$ where $\Delta\phi$ is the azimuthal angle difference between the lepton and the $E_T^{miss}$.

GeV and with a dilepton invariant mass satisfying $m_{ll} > 40$ GeV. Finally, the photon must be separated from the leptons by at least $\Delta R(l,\gamma) > 0.7$. The primary backgrounds to these processes are a $W$ or a $Z$ boson produced in association with jets, where the jet fakes a photon or a charged lepton. The cross section for these processes is measured within the fiducial phase space for both exclusive (0-jet) events and inclusive events. The exclusive cross section measurements can be found in Table 1.

The production of two $W$ bosons of opposite charge has been measured at ATLAS in the case that both $W$ bosons decay leptonically [5]. The leptons are required to have $p_T > 20$ GeV, the dilepton invariant mass of SFOC lepton pairs must be larger than 15 GeV and not be within 15 GeV of the $Z$ mass, and the events must have a large relative missing energy[3]. These cuts are designed to reject background $Z$ events produced in association with jets. In addition, selected events must have no jets with $p_T > 25$ GeV, and no jets with $p_T > 20$ GeV that contain a $b$-hadron. The jet veto is designed to reject background events containing top quarks. The measured cross section can be found in Table 1, and the $p_T$ distribution of the dilepton pair in selected events can be found in the left plot of Figure 1.

The process in which a $W$ and $Z$ boson are produced simultaneously and both decay leptonically to a three lepton final state has also been measured at ATLAS [6]. Three leptons with $p_T > 15$ GeV are required, and the SFOC lepton pair with an invariant mass closest to the $Z$ mass is selected as the $Z$ candidate. The lepton pair invariant mass is required to be within 10 GeV of the $Z$ mass. The events are required to have $E_T^{miss} > 25$ GeV, and the transverse mass calculated with the unpaired lepton and the $E_T^{miss}$ must satisfy $m_T > 20$ GeV. The primary backgrounds to the $WZ$ process are events with two $Z$ bosons, events with a $Z$ produced in association with a jet, and top pair events. The measured cross section can be found in Table 1, and the distribution of the transverse momentum of the $Z$ candidate in selected events can be found in the middle plot of Figure 1.

The simultaneous production of two $Z$ bosons has been measured at ATLAS in the case when both $Z$ bosons decay to electrons or muons [7] resulting in a four lepton ($ZZ \to llll$) final state, and in the case with one $Z \to ll$ decay and the other Z decays to two neutrinos [8] resulting in a final state with two leptons and missing energy ($ZZ \to ll\nu\nu$). In the $ZZ \to llll$ case, all leptons must have $p_T > 7$ GeV, and are required to form two SFOC lepton combinations with masses within 25 GeV of the $Z$ mass. The backgrounds in the four lepton case are small. In the $ZZ \to ll\nu\nu$ case, SFOC leptons must have $p_T > 20$ GeV and have a lepton pair invariant mass within 15 GeV of the $Z$ mass. $ZZ \to ll\nu\nu$ events must also have zero jets in the event, a large axial missing energy[4], and $|E_T^{miss} - p_T^{ll}|/p_T^{ll} < 0.6$ where $p_T^{ll}$ is the transverse momentum of the $Z$ candidate. The distribution of the transverse mass of both leptons and the $E_T^{miss}$ in selected events can be found in the right plot of Figure 1. The remaining backgrounds

---

[3] Relative missing energy is defined as $E_{T,\,rel}^{miss} = \sin(\Delta\phi) \times E_T^{miss}$ for $\Delta\phi > \pi/2$, where $\Delta\phi$ is measured between the missing transverse energy and the nearest lepton or jet. For $\Delta\phi < \pi/2$, the nominal $E_T^{miss}$ is used.

[4] Axial missing energy is defined as $E_{T\ axial}^{miss} = \cos(\Delta\phi) \times E_T^{miss}$ where $\Delta\phi$ is the azimuthal angle difference between the missing transverse energy and the momentum of the lepton pair.

after selection are $WZ$, $WW$, top pairs, and $Z$ produced in association with jets. The measured cross sections for these processes can be found in Table 1.

In all diboson analyses, production cross section measurements are seen to be in agreement with the Standard Model. More details on these analyses can be found in the references listed in Table 1.

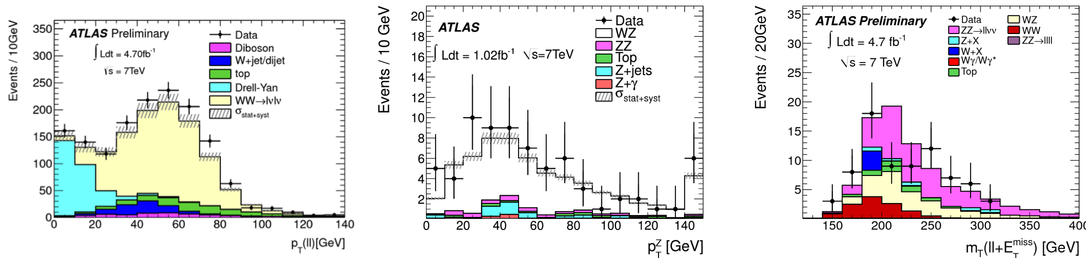


**FIGURE 1.** Left: Transverse momentum of dilepton pairs in $WW$ events [5] . Middle: Transverse momentum of $Z$ candidates in $WZ$ events [6]. Right: Transverse mass of both leptons and the $E_T^{miss}$ in $ZZ \to ll\nu\nu$ events [8].

**TABLE 1.** Summary table of fiducial cross section ($\sigma_{fid}$) and total cross section ($\sigma_{tot}$) measurements for each of the diboson process. Exclusive cross sections are listed for the $W\gamma$ and $Z\gamma$ processes.

| Process | $\int \mathscr{L}$dt | $\sigma_{fid}$ | (stat.) | (syst.) | (lumi.) | $\sigma_{tot}$[pb] | (stat.) | (syst.) | (lumi.) | Reference |
|---|---|---|---|---|---|---|---|---|---|---|
| $W\gamma \to l\nu\gamma$ | 1 fb$^{-1}$ | 3.32 | $\pm$0.10 | $\pm$0.48 | $\pm$0.12 pb | | - | | | [4] |
| $Z\gamma \to ll\gamma$ | 1 fb$^{-1}$ | 1.05 | $\pm$0.04 | $\pm$0.12 | $\pm$0.04 pb | | - | | | [4] |
| $WW \to l\nu l\nu$ | 5 fb$^{-1}$ | | by decay channel | | | 53.4 | $\pm$2.1 | $\pm$4.5 | $\pm$2.1 | [5] |
| $WZ \to l\nu ll$ | 1 fb$^{-1}$ | 102 | $^{+15}_{-14}$ | $^{+7}_{-6}$ | $\pm$4 fb | 20.5 | $^{+3.1}_{-2.8}$ | $^{+1.4}_{-1.3}$ | $^{+0.9}_{-0.8}$ | [6] |
| $ZZ \to llll$ | 5 fb$^{-1}$ | 21.2 | $^{+3.2}_{-2.7}$ | $^{+1.0}_{-0.9}$ | $\pm$0.8 fb | 7.2 | $^{+1.1}_{-0.9}$ | $^{+0.4}_{-0.3}$ | $\pm$0.3 | [7] |
| $ZZ \to ll\nu\nu$ | 5 fb$^{-1}$ | 12.2 | $^{+3.0}_{-2.8}$ | $\pm$1.9 | $\pm$0.5 fb | 5.4 | $^{+1.3}_{-1.2}$ | $^{+1.4}_{-1.0}$ | $\pm$0.2 | [8] |

## LIMITS ON ANOMALOUS TRIPLE GAUGE COUPLINGS

New physics that interacts with the electroweak sector but exists at an energy scale not directly probed by LHC energies may cause deviations of triple gauge boson couplings from Standard Model predictions. These anomalous triple gauge couplings (aTGC) are modeled using an effective Lagrangian approach [9], and are predicted to cause deviations in the cross sections and kinematic distributions of diboson processes. For each diboson measurement, the event yield or a kinematic distribution of the selected sample is used to set limits at the 95% Confidence Interval (C.I.) on the size of aTGCs using 1 fb$^{-1}$ of 2011 data. In the left plot of Figure 2, the leading lepton $p_T$ distribution in $WW$ events is shown, as well as the expected deviations of this distribution in the presence of aTGCs. Limits derived on aTGCs in the $W\gamma$ and $ZZ \to llll$ analyses can be found in the middle and right plots of Figure 2, respectively. Table 2 summarizes the limits derived on anomalous couplings from each diboson analysis, where each coupling is associated to a term in the effective Lagrangian and indicates a deviation from the Standard Model. References with more details on these limits can be found in the table.

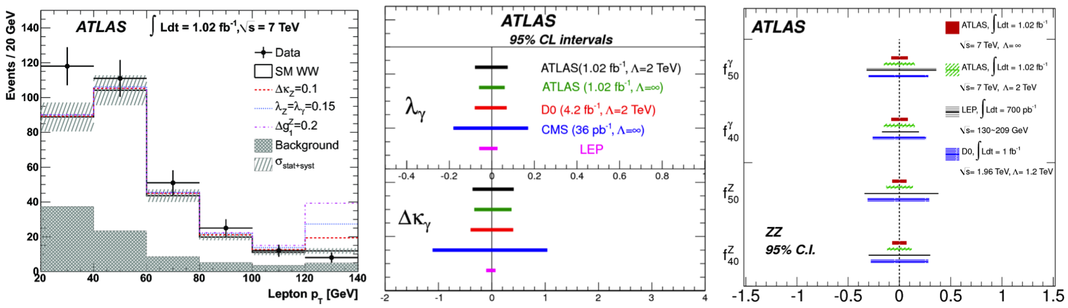


**FIGURE 2.** Left: leading lepton $p_T$ distribution used for aTGC limit setting in $WW$ events [10]. Middle: Limits at the 95% C.I. on aTGCs in $W\gamma$ events [4]. Right: Limits at the 95% C.I. on aTGCs in $ZZ \to llll$ events [11].

**TABLE 2.** Summary table of limits at the 95% C.I. on anomalous couplings from each of the diboson measurements. All listed limits use a form factor scale of $\Lambda = \infty$ [9]. Dashes indicate that the analysis is not sensitive to that aTGC. It should be noted that the limits from the $WW$ analysis are derived using the LEP constraint [10].

| Coupling | $W\gamma \to l\nu\gamma$ [4] | $Z\gamma \to ll\gamma$ [4] | $WW \to l\nu l\nu$ [10] | $WZ \to l\nu ll$ [6] | $ZZ \to llll$ [11] |
|---|---|---|---|---|---|
| $\Delta\kappa_\gamma$ | $[-0.33, 0.37]$ | - | - | - | - |
| $\lambda_\gamma$ | $[-0.060, 0.060]$ | - | - | - | - |
| $\Delta g_1^Z$ | - | - | $[-0.052, 0.082]$ | $[-0.16, 0.24]$ | - |
| $\Delta\kappa_Z$ | - | - | $[-0.071, 0.071]$ | $[-0.8, 1.0]$ | - |
| $\lambda_Z$ | - | - | $[-0.079, 0.077]$ | $[-0.14, 0.14]$ | - |
| $h_3^Z$ | - | $[-0.022, 0.026]$ | - | - | - |
| $h_3^\gamma$ | - | $[-0.028, 0.027]$ | - | - | - |
| $h_4^Z$ | - | $[-0.00022, 0.00021]$ | - | - | - |
| $h_4^\gamma$ | - | $[-0.00021, 0.00021]$ | - | - | - |
| $f_{50}^Z$ | - | - | - | - | $[-0.07, 0.07]$ |
| $f_{50}^\gamma$ | - | - | - | - | $[-0.08, 0.08]$ |
| $f_{40}^Z$ | - | - | - | - | $[-0.07, 0.07]$ |
| $f_{40}^\gamma$ | - | - | - | - | $[-0.08, 0.08]$ |

# REFERENCES

1. ATLAS Collaboration, *JINST* **3 S08003** (2008).
2. L. Evans and P. Bryant (editors), *JINST* **3 S08001** (2008).
3. M. Cacciari, G. P. Salam, and G. Soyez, *JHEP* **04:063** (2008).
4. ATLAS Collaboration, arXiv:1205.2531 [hep-ex], submitted to Phys. Lett. B (2012).
5. ATLAS Collaboration, ATLAS-CONF-2012-025, http://cdsweb.cern.ch/record/1430734 (2012).
6. ATLAS Collaboration, *Phys. Lett.* **B 709**, 341 (2012).
7. ATLAS Collaboration, ATLAS-CONF-2012-026, http://cdsweb.cern.ch/record/1430735 (2012).
8. ATLAS Collaboration, ATLAS-CONF-2012-027, http://cdsweb.cern.ch/record/1430736 (2012).
9. K. Hagiwara, R. D. Peccei, and D. Zeppenfeld, *Nucl. Phys. B* **282**, 253 (1987).
10. ATLAS Collaboration, *Phys. Lett.* **B 712**, 289 (2012).
11. ATLAS Collaboration, *Phys. Rev. Lett.* **108**, 041804 (2012).